LA-UR-12-23675
Approved for public release; distribution is unlimited.

Title:	Preshot Predictions for Defect Induced Mix (DIME) Capsules
Author(s):	Bradley, Paul A. Krasheninnikova, Natalia S. Tregillis, Ian L. Schmitt, Mark J.
Intended for:	Archival document

Los Alamos
NATIONAL LABORATORY
EST. 1943

memorandum

Computational Physics Division
Plasma Theory and Applications XCP-6)

To/MS: distribution
From/MS: P.A. Bradley, N. Krasheninnikova, I. Tregillis, and M.J. Schmitt

Phone/Fax: 7-8999/FAX 5-6722
Symbol: LA-UR-12-00XXX
Date: July 20, 2012

SUBJECT: ***Preshot predictions for Defect Induced Mix (DIME) capsules***

Introduction

In this memo, we evaluate the most probable yield and other results for the Defect Induced Mix (DIME-12A) Polar Direct Drive (PDD) capsule-only shots. We evaluate the expected yield, bang time, burn averaged ion temperature, and the average electron temperature of the Ge line-emitting region. We also include synthetic images of the capsule backlit by Cu K-α emission (8.39 keV) and core self-emission synthetic images. This memo is a companion to the maximum credible yield memo (LA-UR-12-00287) published earlier.

The Capsule and Experiment Requirements

The capsule we propose to shoot on the NIF has an outer radius of 1100 μm, a shell thickness of 42 μm, and nominal gas fill of 5 atm D_2. From inside to outside, the capsule will consist of a 2 μm layer of 1.5 atom% Ge-doped CH plastic with the outer 40 μm being pure CH plastic. The first capsule design will be a spherical shell, while the second capsule will have a 10 μm deep by 80 μm wide groove around the equator. In Figure 1, we show a schematic of the capsule in the left panel, while the right panel of Figure 1 shows one of our NIF capsules at General Atomics with the groove and fill tube.

One thing that is essential for shots on the NIF are the experimental requirements. We have the following: 1) Yield; 2) bangtime; 3) Measurement of radius at a given time from backlit images for the radius versus time plot; 4) Capsule symmetry as seen from the equatorial backlighter; 5) capsule symmetry as seen from the polar self-emission images. Note that these requirements define whether or not the experiment was successful and does not necessarily correlate with the expected capsule performance. For the yield (#1), we need to be able to obtain a useful yield from the neutron detectors and radiochemistry. We set this at 10^{10} neutrons. We need to measure the bangtime (#2) accurately enough to tell if there is a significant difference between defect and non-defect capsules. We also need to calibrate our source to predict the correct bangtime for the expected laser drive. A measurement to within +/- 50 ps is required. For the radius at a given time (#3), we need to be able to measure it to within +/- 20μm for a given point. We set a pole/equator radius ratio (#4) for the equatorial

backlighter view. Our simulations indicate that we need a pole/equator ratio between 0.7 and 1.5 to see the groove at the 25% radius time. Note that this implies we can tolerate a pancaked image more than a sausage shaped image. We extend this requirement to need a $\Delta r/r$ of 50% in any direction except in the equatorial plane when a groove is present. Finally, we require no more than a $\Delta r/r$ of less than +70% in the polar self- emission image, which is set by the expected perturbation caused by losing a quad in one of the 44.5° or 50° drive beams.

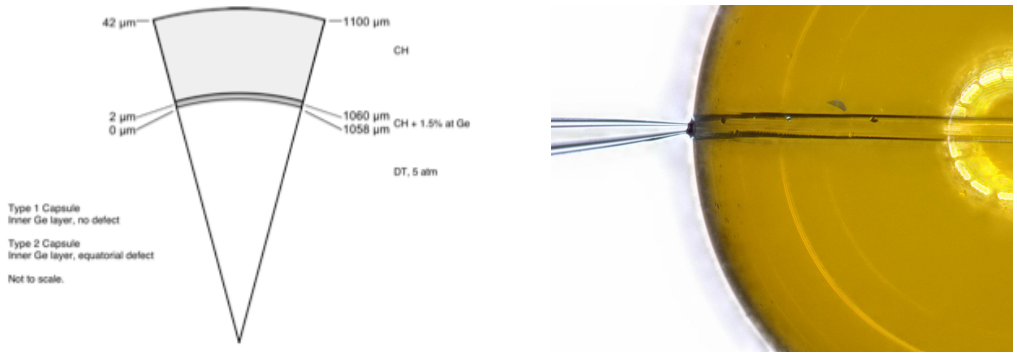

Figure 1: A schematic of the dopant configuration of the DIME-12A capsule (left panel) showing the 2 µm thick dopant layer with 1.5 atom% Ge in the CH plastic. The right panel shows an actual DIME-12A capsule with the 10 µm deep by 80 µm wide groove around the equator and a glass fill tube. (The bright circle is the lamp used to illuminate the target.)

Yield, bang time, and ion temperature

Our expected yield will be much less than the clean 1-D yield of 1.8×10^{14} neutrons computed in the maximum credible yield memo. This is based on our experience with smaller capsules fielded on the Omega laser and LLE's shots done on NIF in 2011. We have four methods of computing the most likely yield and all predict yields for perfect DIME capsules near 10^{12} DD neutrons. As an aside, we note that our Eulerian simulations with mix predict about 50 ng of Ge will mix into the gas before bang time. After bang time, the amount of Ge in the gas increases to about 300 ng. For comparison, a very preliminary mix calculation of a NIC symcap predicts about 40 ng of Ge mixed into the gas before bang time and about 700 ng of Ge after bang time.

Our first relevant example of expected yield determination is based on shots N110617 and N120217. These were ~700 kJ PDD capsules designed to test the neutron imaging spectrometer. The actual yields were 6.8 and 5.8 +/-0.1x10^{14} neutrons, and the quoted LLE YOC was ~6%. We ran 1-D Lasnex and 1-D Eulerian calculations of these shots and obtained yields of ~7.5x10^{15} neutrons. Our YOC is 8 to 9%, within 50% of the LLE results. We also computed the yield using our Eulerian code with mix turned on and the prediction is 3.0x10^{15} neutrons, for yield-over-mix ratios of 0.23 and 0.19, which are comparable to what we obtained for our previous Omega shots. Thus, we

would take our 1-D (with mix) yield prediction for our NIF capsule ($3.4x10^{12}$ neutrons) and scale it by 0.20 to 0.25 for an estimate of 6.8 to $8.5x10^{11}$ neutrons. Our estimated mass averaged ion temperature (Tion) value is 7.8 keV, which is 1.2 keV lower than the experimental value. The burn-averaged temperature is 11 keV, and our being 2 keV higher than the data is consistent with our earlier results for Omega capsules. Given that our proposed shot is also with PDD, we would expect roughly the same degradation in yield and Tion.

The second relevant example also makes use of shots N110617 and N120217. These capsules utilized 10 atm of DT gas and the 10 μm glass + 20 μm CH ablator has almost an identical mass to our 42 μm CH ablator. We can thus obtain a crude yield estimate for our capsules by accounting for the difference in D_2 vs DT cross section (about a factor of 100) and the difference in gas fill by scaling the number of atoms available to react (a factor of 2). This scaling would suggest reducing the observed yield of the LLE capsules by a factor of 200, and the resulting yield estimate would be 2.9 to $3.4x10^{12}$ neutrons.

We also used a YOC scaling of 0.08 to 0.09 on clean 1-D simulations of our capsules. Our clean 1-D simulation has a yield of $1.8x10^{14}$ neutrons and if we use a YOC of 0.08 from the LLE capsules described in the previous paragraph, we also obtain a predicted yield of $1.4x10^{13}$. Given that this estimate has the largest extrapolation and disagrees with all the other estimates, we place less weight on this estimate.

The next relevant example is our preshot calculations of our NIF capsule design that do and do not have turbulent mix included. We computed several 1-D and 2-D runs with and without mix. Our 1-D Eulerian simulation yields (with mix) produce about $3.4x10^{12}$ neutrons. The equivalent 2-D simulation has a yield of $3.1x10^{12}$ neutrons. Finally, P. McKenty of LLE ran a calculation of our capsule using a fall-line mix prescription and obtained a yield of $2.2x10^{12}$ neutrons; this estimate is good to within a factor of two. In short, all of our simulations predict the yield should be about $3x10^{12}$. However, with our Omega capsule shots, we found that the Eulerian code predictions were about a factor of roughly 4 higher than the data. If we account for this, we derive an expected yield of $\sim 10^{12}$ neutrons. Our predicted Tion values are 5 keV (mass averaged) and 8.4 keV (burn averaged). Our experience with Omega capsules suggests we add about 1 keV to the mass averaged result and subtract about 2 keV from the burn-averaged result to obtain the experimental value. In both cases, we determine a value of ~6 keV for the experimental burn averaged ion temperature.

All four examples suggest an expected yield for our perfect capsules of 10^{12} neutrons. We assign a probable factor of three spread ($3x10^{11}$ to $3x10^{12}$ neutrons) in yield to account for modeling uncertainties. These modeling uncertainties include (but are not limited to) the range in possible gas fills from 4 to 6 atm and its effect on yield, which is +/- 45%, and a +/- 20% change in yield from a +/- 3 μm change in capsule shell thickness. We have included the effect of the fill tube in some of our calculations. We find that the yield is reduced by 10 to 15%, while the bang time, burn temperature, and

burn width are negligibly affected. Our calculated results when we also included a glue spot were nearly identical to the case with the fill tube alone. We obtained target metrology in June 2012 and find that the capsules have a diameter 50 μm larger than the nominal 2200 μm. We ran calculations with the larger diameter and the average ablator thickness of 41.5 μm (spec was 42 μm), and find that the yield increased by 15%. The net result is the fill tube and larger capsule diameter simulated yields cancel each other out in predictions of capsule performance.

Our capsules with an 80 μm wide by 10 μm deep defect produce calculated yields that are a factor of 20 lower than the perfect capsule. However, we find that the Omega experimental yields from defect capsules are a factor of 4 to 8 higher than the calculated yields. This is because the shock breaking out of the groove is too strong, which disrupts the capsule too much and lowers the yield too much. Our Omega data shows that 15 to 17 μm thick shell capsules with grooves produce yields that are a factor of only 2 to 3 lower than the perfect capsules. We believe this will also be the case for the NIF capsule, and this implies a yield of about $3x10^{11}$ neutrons. We ran calculations with 5x80 μm and 20x80 μm grooves as part of the design process and to assess the yield sensitivity to groove dimensions. The results are shown in Table 1. The estimated yields consider the trends simulated versus experimental yield from the September 2009 and January 2011 shots. In addition, we found that the 5x80 μm groove calculation, as well as calculations with shallower or narrower grooves did not show enough change in the x-ray images between the groove and no groove case. Simulated backlit mages from simulations with 10x80 μm (see Figure 2) and 20x80 μm grooves show considerable difference from the no groove case, but the 20x80 μm simulation has a large drop in yield compared to the 5x80 μm and no groove case. The best compromise for yield and backlit image difference is a 10x80 μm groove. We assign a factor of three uncertainty in yield to our yield prediction, resulting in a spread of 10^{11} to 10^{12} neutrons.

TABLE 1: Summary of simulated and estimated yields for capsules with grooves

Capsule type	Calculated yield	Expected yield
No groove	$3.1x10^{12}$	$\sim10^{12}$
5 μm deep by 80 μm wide	$4.2x10^{11}$	$\sim8x10^{11}$
10 μm deep by 80 μm wide	$1.5x10^{11}$	$\sim3x10^{11}$
20 μm deep by 80 μm wide	$0.2x10^{11}$	$\sim0.7x10^{11}$

One thing we examined in response to questions raised in the readiness review dealt with the timing and yield associated with the shock hitting the capsule center for the first time. We found that the shock hits the center at about 2.8 ns, 400 ps before bang time. The yield at this point is between 10^{-4} and 10^{-3} of the total, or less than 10^{9} neutrons. We examined simulations of capsules with different thicknesses; we do not see evidence of a significant yield peak associated with the first shock hitting the center unless the CH shell is about 15 μm. Even then the yield associated with the first shock is only 10^{-5} of the total.

We also predict the bang time and estimate the error in this value for purposes of diagnostic timing. We took calculations for three different computer codes for the same

capsule and derive a value of 3.18 +/- 0.09 ns. This does not include additional uncertainties due to changes in capsule thickness, gas fill, or capsule size. We considered their effect and they are: +/- 1 atm change (+/- 20 ps); +/- 3 μm thickness (176 ps and the largest by far); +/- 20 μm in diameter (+/- 19 ps). When we add these uncertainties (and the code uncertainty) in quadrature, the bang time uncertainty is +/- 200 ps, for a value of 3.18 +/- 0.20 ns. We must note that in reality, we will know the capsule diameter and shell thickness before we shoot the capsule, so the actual uncertainty in bang time will be much closer to the value with the code uncertainty, namely 3.18 +/- 0.10 ns. We will use this as the official value.

We postprocessed Eulerian and Lagrangian simulations for our estimates of burn-averaged ion and electron temperatures. We computed a mass average burn temperature of 5.1 keV and a burn averaged temperature of 8.4 keV. Scaling these from our comparison to the LLE designed capsules suggests values of 6.3 keV and 6.4 keV. For the perfect capsule, we estimate a burn-averaged ion temperature of 6.0 to 6.5 keV. The electron temperature is of interest for the spectrometer images and our prediction is ~5 keV. We predict a burn width of 250 +/- 30 ps. For the defect capsule, we expect an average ion temperature about 0.2 keV lower than the perfect capsule, for a prediction of 5.8 keV. Likewise, we expect the electron temperature to be about 0.2 keV lower, for a prediction of ~4.8 keV. The predicted burn width is 430 +/- 60 ps. Unfortunately, there will not be a burn width measurement.

In summary, comparisons of simulations to Omega data, predictions for our upcoming NIF capsules, and Omega experimental trends all point to an expected yield of ~10^{12} neutrons for the perfect capsules and about 3x10^{11} neutrons for capsules with a 80 μm wide by 10 μm deep defect. We predict a burn averaged ion temperature of 4 to 5 keV and a burn width of 250 ps. We predict a bang time of 3.2 to 3.3 ns for the perfect capsule and about 2.9 to 3.0 ns for the defect capsule. We present a summary of our predictions in Table 2.

TABLE 2: Summary of integral measurement quantities

Quantity	No Defect	Defect
Yield (DD neutrons)	3x10^{11} to 3x10^{12}	10^{11} to 10^{12}
Bang time (ns)	3.18 +/- 0.10	3.00 +/- 0.15
Burn averaged Ti (keV)	~6 to 6.5	~5.8 to 6.3
Burn averaged Te (keV)	~5	~4.8

Backlit images

We expect to obtain backlit images of the imploding capsule at about ½ the initial radius, ¼ the initial radius, and near bang time. We will use a V backlighter (line is at 5.205 keV) and the images will be recorded with the 90-78 hGXI imager. Our first example images (see Figure 2) come from an Eulerian code calculation that includes the

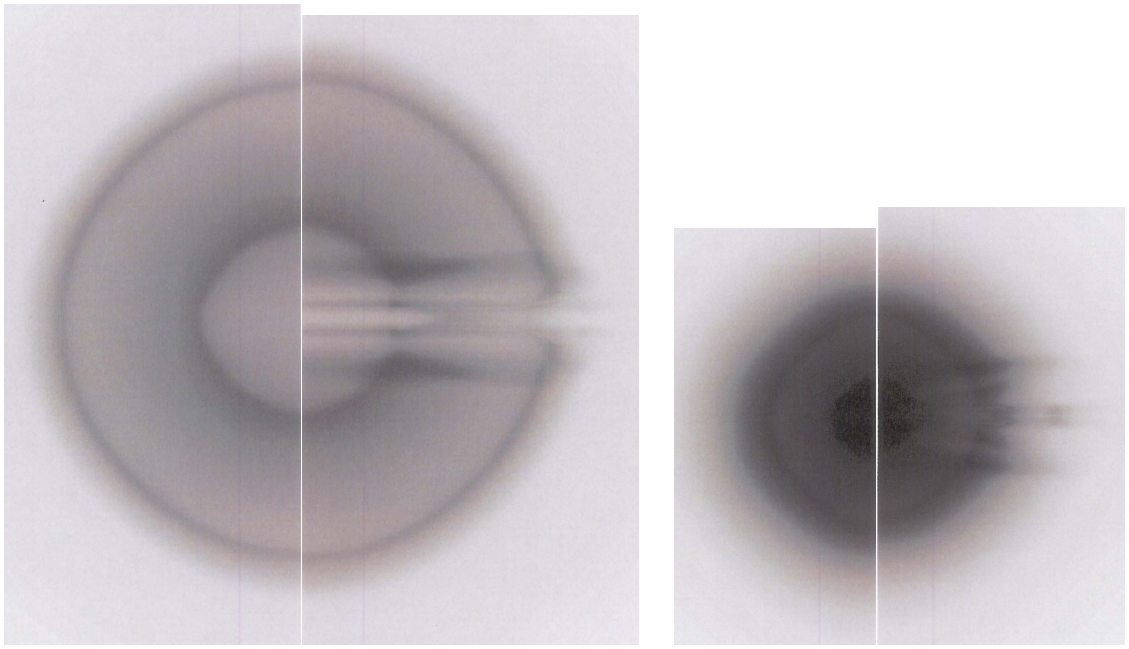

Figure 2: Simulated V backlighter absorption images of the DIME 12A capsule at ~1/2 radius (2.2 ns, left panel), ~1/4 radius (2.75 ns, right panel). The equator runs through the center of each image. Each simulated image consists of a perfect capsule image on the left side and a 10μm deep by 80 μm wide groove on the right side.

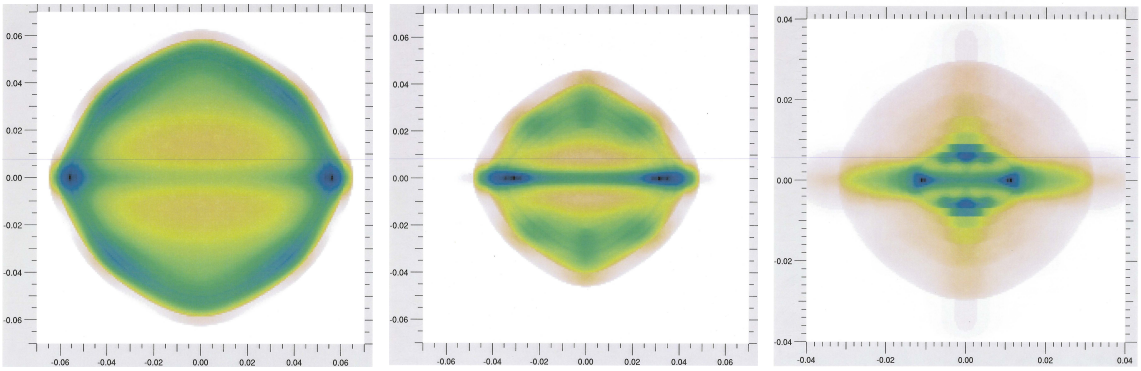

Figure 3: Simulated Hydra V backlighter absorption images of the non-defect DIME 12A capsule at ~1/2 radius (2.3 ns, left panel), ~1/4 radius (2.6 ns, center panel), and near bang time (about 3.0 ns, right panel). The equator runs horizontally through the center of each image. The frames are 1400 μm across on each side for the first two images and 800 μm across on each side for the last image.

effects of polar direct drive. The simulated image radii are ~580 μm at 2.2 ns (~1/2 radius), ~280 μm at 2.75 ns (~1/4 radius), and ~110 μm at 3.1 ns (near bang time). We do not show images near bang time, since the imploded core is essentially opaque to the

V backlighter. At ¼ radius and near bang time, there is noticeable edge darkening due to the increasing optical depth of the Ge dopant. There is a small difference between the polar and equatorial radii due to the angular drive asymmetry.

We also computed synthetic backlit images using Hydra (see Figure 3) and Lasnex, (see Figure 4) both of which include the PDD pointing effects. The images shown in this section include the effect of the kapton filter and photocathode detector response function, which limits the transmitted energies to greater than 4 keV. This, coupled with the optical depth of the capsule at late times requires us to use V for the backlighter. A Legendre mode analysis of the Hydra simulation shows a P_2 asymmetry of 5 to 7% until minimum radius, when the value drops to nearly 15% (see Figure 5). The drive asymmetry becomes more pronounced as the implosion progresses, with the equator being about 30% wider near bang time (see Figure 3). Near bang time, the image is about 70x100 µm. The time-dependent P_4 and P_8 moments are 3% and 10% respective at ½ radius, while at ¼ radius, P_4 and P_8 are ~6%. The rapid changes in symmetry in Figure 5 occur near the bang time of ~3 ns. The Lasnex images show a 5 to 10% pancake asymmetry between ½ radius and ¼ radius (see Figure 4). Thus, all three codes show similar P_2/P_0 behavior. We also have lineouts (not shown here) to show the specific intensity. Between ½ radius and ¼ radius, the specific intensity is between 1.7 $x10^{-7}$ and $1.3x10^{-7}$ jk/cm^2/keV/ster. Near bang time, the *minimum* specific intensity drops to below $1.0\ x10^{-7}$ jk/cm^2/keV/ster.

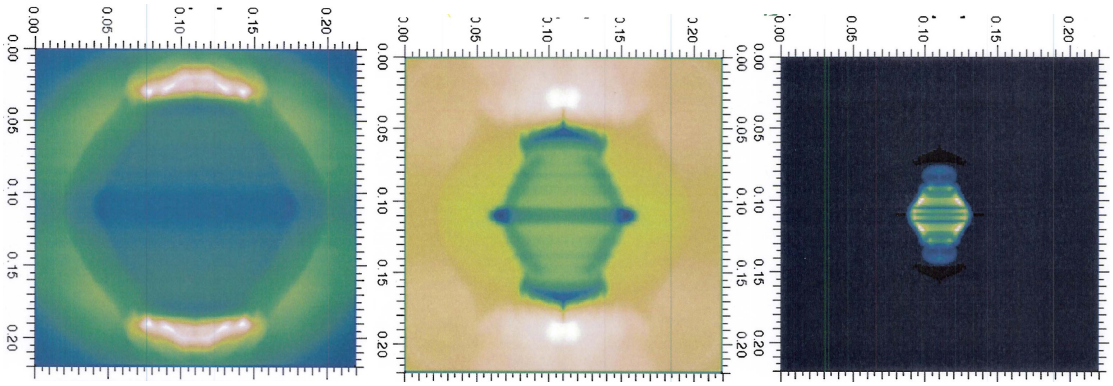

Figure 4: Simulated Lasnex V backlighter absorption images of the DIME 12A capsule at ~1/2 radius (2.31 ns, left panel), ~1/4 radius (2.76 ns, center panel), and near bang time (right panel). The equator runs horizontally through the center of each image. The frames are 2000 µm across on each side.

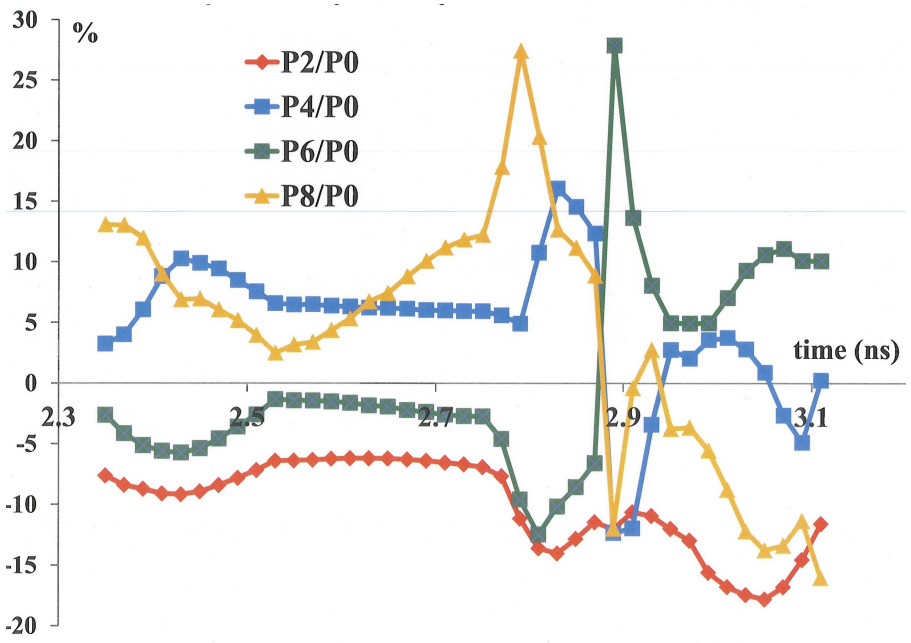

Figure 5: Simulated P_2/P_0, P_4/P_0, P_6/P_0, and P_8/P_0 from the Hydra code.

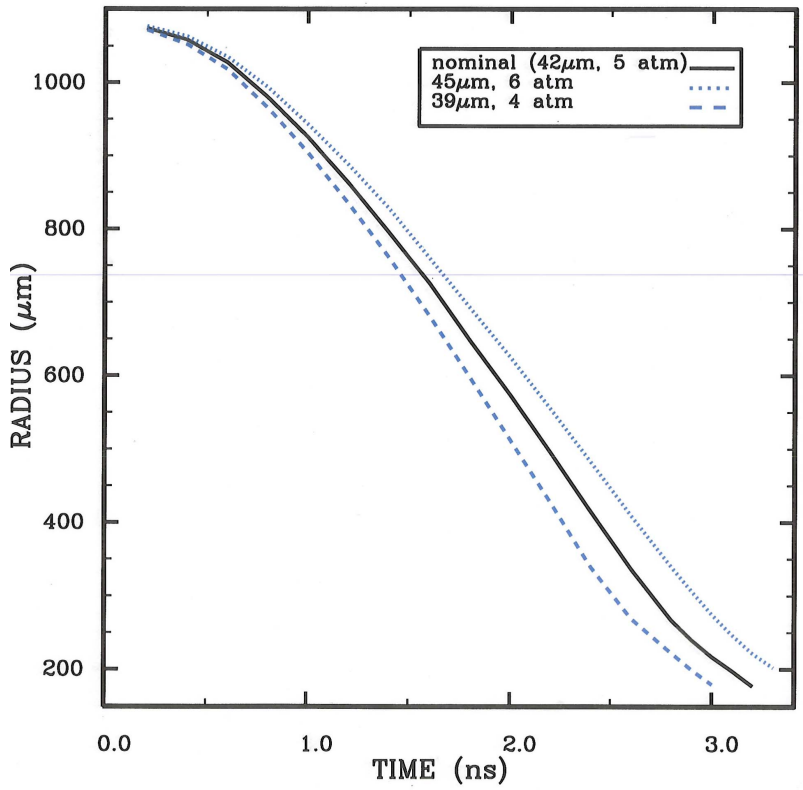

Figure 6: Simulated radius versus time trajectory from a 1-D simulation.

The predicted radius versus time plot for a nominal (42 μm shell, 5 atm fill, 700 kJ) drive defect-free capsule is shown in Figure 6, along with trajectories for an extreme slow possibility (45 μm shell, 6 atm gas fill and 665 kJ) capsule (dotted line) and an extreme fast possibility (39 μm shell, 4 atm gas fill and 735 kJ) capsule (dashed line).

The nominal curve reaches approximately ½ radius at 2.2 ns, and the maximum spread in radius at this point is +/- 55 µm. At ¼ radius (2.8 ns), the spread is +70/-45 µm. However, we expect the actual uncertainty in radius due to changes in implosion velocity to be about half what we state, since we will know the thickness of the capsule shell well ahead of the shot. Based on experience with Omega, we expect the radius measurement error from the data to be less than 5 µm. This is about 1/5 our expected implosion uncertainty, so we will be able to easily constrain our source model for the capsule. The bang time is 3.2 +/- 0.2 ns, in agreement with our estimate presented earlier.

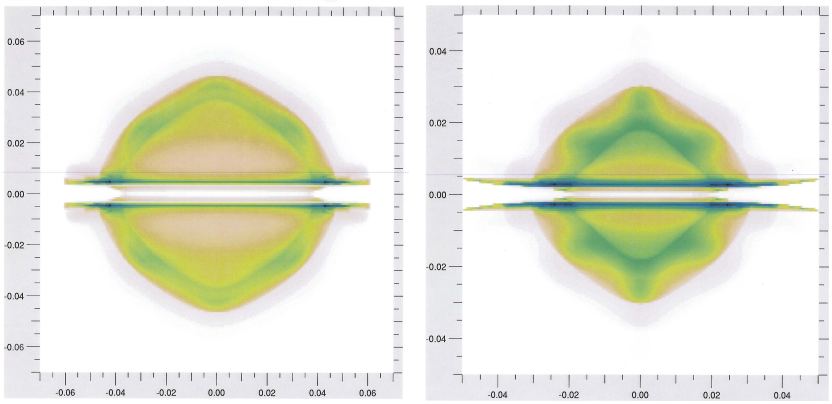

Figure 6: Simulated Hydra V backlighter absorption images of the DIME 12A groove capsule at ~1/2 radius (2.3 ns, left panel) and ~1/4 radius (2.6 ns, right panel). The equator runs horizontally through the center of each image. The frames are 1400 µm across on each side for the first image and 1000 µm across on each side for the second image.

Finally, we have Hydra simulations of a capsule with a 10x80 µm groove. The Hydra simulation predicts a groove width of ~100 to 110 µm at ½ radius and about 70 µm at ¼ radius (see Figure 6). These values are similar to our Eulerian code results, which were shown in Figure 2.

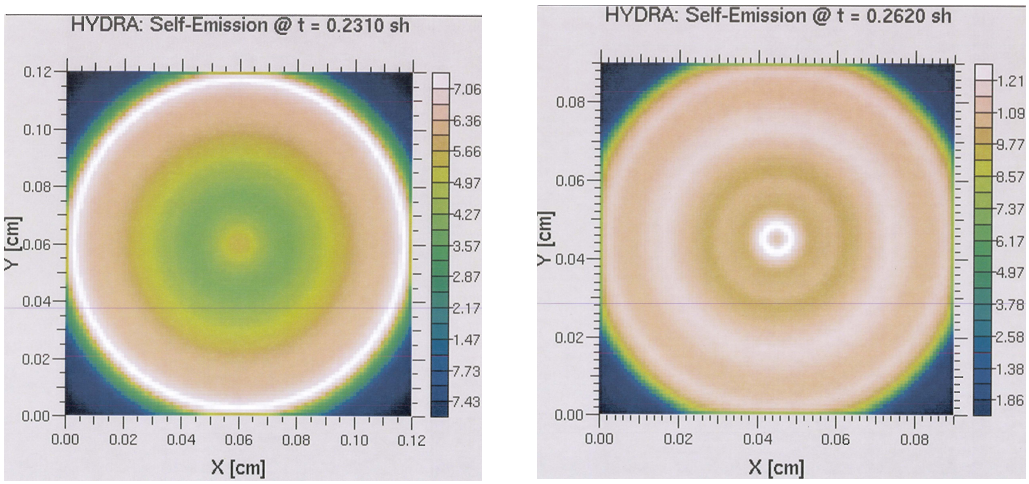

Figure 7: Simulated Hydra self-emission images of the DIME 12A capsule at ~1/2 radius (2.31 ns, left panel), and~1/4 radius (about 2.62 ns, right panel). These

views are from the pole, consistent with the location of the (0-0) hGXI diagnostic. The frames are 1200 µm across (left) and 900 µm (right) on each side.

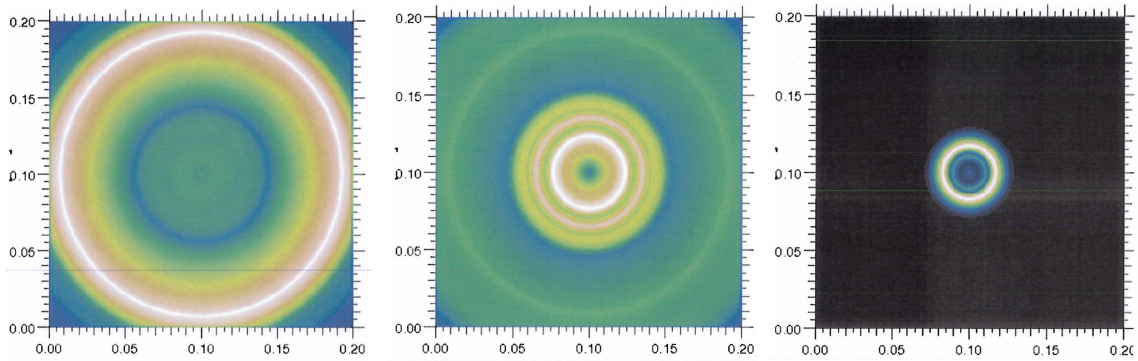

Figure 8: Simulated Lasnex self-emission images of the DIME 12A capsule at ~1/2 radius (2.12 ns, left panel), ~1/4 radius (2.45 ns, center panel), and near bang time (about 3.2 ns, right panel). These views are from the pole, consistent with the location of the (0-0) hGXI diagnostic. The frames are 2000 µm across on each side.

Self-emission images

We plan to record self-emission images of the capsule using the polar (0-0) hGXI imager. Our simulated images from an Eulerian code (that neglects PDD effects) predict an average radius of ~110 µm. Because the capsule groove is in the equatorial plane, we will not see the effect of the groove.

We also have Hydra (see Figure 7) and Lasnex self-emission images. We considered the entire energy range from 0.1 to 14.9 keV, although in practice only the energies from ~5 to about 15 keV will be recorded due to the convolution of the Kapton filter and detector response. We also show normalized Lasnex images in Figure 8 for three different times. The ½ radius images show a relatively bright "ring" at about 575 µm in radius. The ¼ radius images show a bright ring about 50 µm in radius with fainter rings outside of this in Hydra, while Lasnex predicts a bright ring at 250 µm. This will provide an interesting point of comparison. The images at ½ radius have peak emission fluxes of $8x10^{-12}$ jk/cm^2/keV/ster. At ¼ radius, the peak emission fluxes are 4 to $6x10^{-11}$ jk/cm^2/keV/ster. Near bang time, the flux jumps up to $3x10^{-11}$ jk/cm^2/keV/ster in the simulation. However, these simulations are clean and must be regarded as approximate.

"Playbook" Simulations and Predictions

We have not yet fielded shots on the NIF, therefore we are not certain if the symmetry predicted by our simulations is what we will actually see in the experiment. We have created a "playbook" of simulation symmetry versus pole to equator power balance and beam pointing. If the actual symmetry is much worse than we predict, we

can adjust the NIF laser between shots (scheduled for July 28 and 30, 2012) and make the second shot more symmetric. In Figure 9, we show the effect of changing the power balance of the 23.5° and 30° beams. The P_2 moment shows the largest sensitivity, with a 1% +P_2 change for every 3% reduction in the power of the 23.5° and 30° beams. There is much less sensitivity to changing the power of the 44° and 50° beams and our ability to change the energy is limited by the maximum 2 TW per beam of the NIF. Given that the LLE designed neutron yield shots and the Hydra simulations all indicate a significantly oblate implosion, we anticipate that we may have to reduce the power in the 23.5° and 30° beams. Another alternative is to change the beam pointing, although this requires calculations to assure that the beams do not hit anything and a "blowby" analysis to assure that the amount of laser energy going past the capsule at early times is within acceptable limits. That said, we show the P_2 portion of our pointing change analysis in Figure 10. We see from Figure 10 that we want to move the 42° or 30° cones in the negative direction make P_2 more positive. Although not shown here, such a change will make P_4 less positive, but P_8 more positive. We consider the beam pointing to be an alternate means of controlling P_2 if the needed supplementary analyses and reviews are performed in a timely manner.

Because it is difficult to have a beam power or pointing change done at the last minute in NIF, we have a pre-loaded plan for changing the symmetry if needed. Our requirement is that the equatorial radius be less than twice the polar radius. If this requirement is not met, we will reduce the power on the 23.5° and 30° cones by 25% before the second shot. For this, we only need the equatorial and polar radii of the 50% contour when the capsule is at ¼ radius with a measurement error of 0.1 on R_pole/R_eq. We anticipate a scanned image of the first shot 6 to 9 hours afterwards.

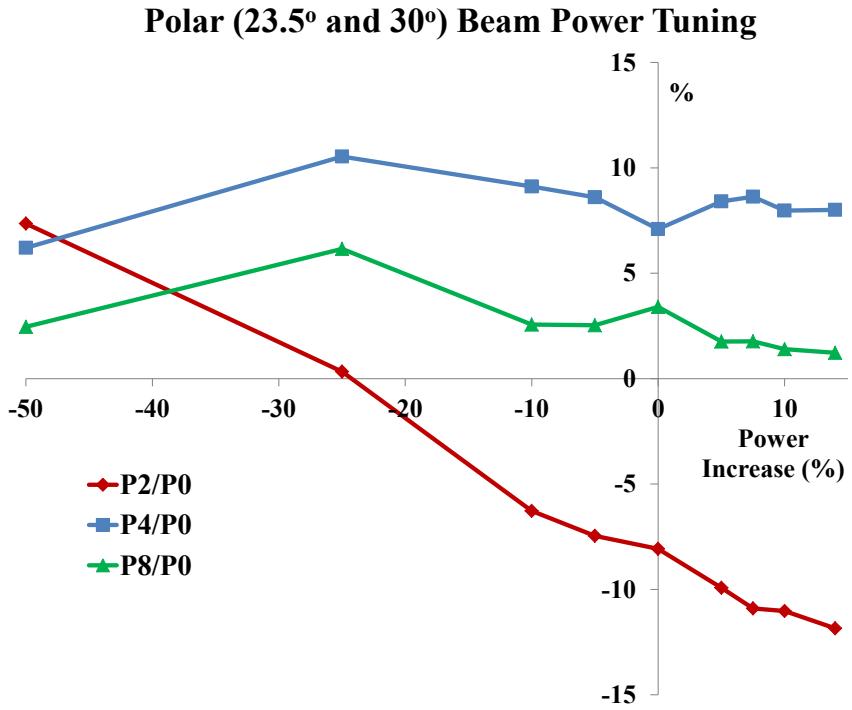

Figure 9: Simulated symmetry changes in Legendre modes 2, 4, and 8 as a result of changing the amount of energy in the 23.5° and 30° beams. For the nominal case, the Hydra simulations predict a -8% P_2, indicating that the capsule will be oblate. Reducing the 23.5° and 30° beam power by ~25% would remove most of the P_2 at the expense of increased P_4 and P_8.

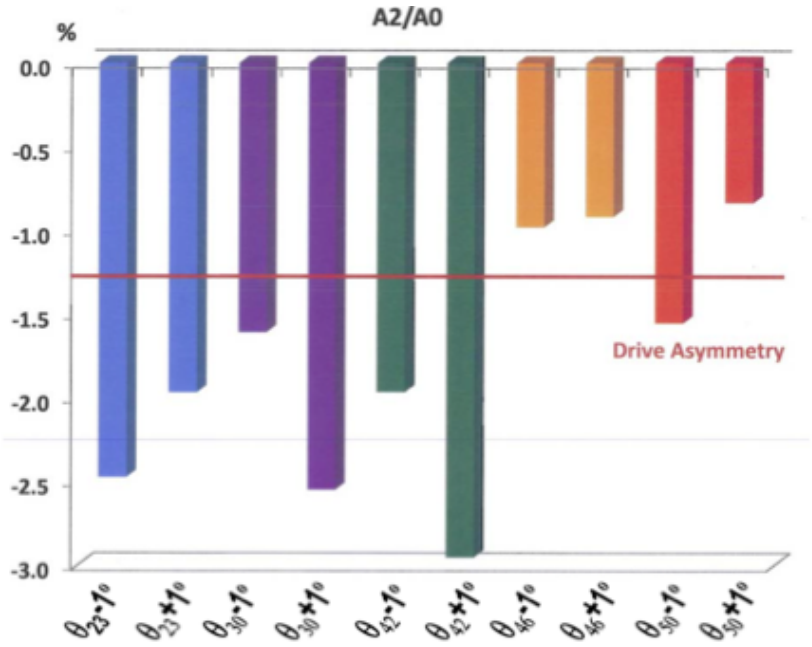

Figure 10: Simulated symmetry changes in Legendre mode 2 as a result of changing the beam pointing on the capsule. Changing the pointing of the 42° beam has the largest effect, although the 23° and 30° beams also change the symmetry.